Hindawi
Journal of Nanomaterials
Volume 2018, Article ID 8148072, 15 pages
https://doi.org/10.1155/2018/8148072

Review Article

Perovskite-Based Solar Cells: Materials, Methods, and Future Perspectives

Di Zhou, Tiantian Zhou, Yu Tian, Xiaolong Zhu, and Yafang Tu

School of Physics & Information Engineering, Jianghan University, Wuhan 430056, China

Correspondence should be addressed to Di Zhou; dizhou@jhun.edu.cn

Received 31 October 2017; Accepted 13 December 2017; Published 15 January 2018

Academic Editor: William Yu

A novel all-solid-state, hybrid solar cell based on organic-inorganic metal halide perovskite ($CH_3NH_3PbX_3$) materials has attracted great attention from the researchers all over the world and is considered to be one of the top 10 scientific breakthroughs in 2013. The perovskite materials can be used not only as light-absorbing layer, but also as an electron/hole transport layer due to the advantages of its high extinction coefficient, high charge mobility, long carrier lifetime, and long carrier diffusion distance. The photoelectric power conversion efficiency of the perovskite solar cells has increased from 3.8% in 2009 to 22.1% in 2016, making perovskite solar cells the best potential candidate for the new generation of solar cells to replace traditional silicon solar cells in the future. In this paper, we introduce the development and mechanism of perovskite solar cells, describe the specific function of each layer, and focus on the improvement in the function of such layers and its influence on the cell performance. Next, the synthesis methods of the perovskite light-absorbing layer and the performance characteristics are discussed. Finally, the challenges and prospects for the development of perovskite solar cells are also briefly presented.

1. Introduction

With increasing global energy consumption and environmental pollution, traditional fossil energy sources cannot meet the sustainable development of human society. The utilisation of clean, renewable energy sources has become a prerequisite for the development of human society. Among a variety of new energy technologies, solar power is undoubtedly one of the most promising technologies. A solar cell is a device that converts light energy directly into electrical energy via photovoltaic effects or photochemical reactions. In 1839, the French physicist Becquerel discovered the photovoltaic effect for the first time. In 1876, British scientists Adams et al. found that a selenium semiconductor could produce electricity when it was radiated under sunlight [1]. In 1883, Fritts successfully prepared the first semiconductor/metal junction solar cell with a piece of germanium coated with a thin layer of gold although the efficiency was only ~1%. In 1954, Pearson et al. from US Bell Labs developed the first piece of crystalline silicon solar cell and achieved a conversion efficiency of 4.5%, thus beginning a new era for the utilisation of solar power [2]. The monocrystalline silicon/polycrystalline silicon solar cells currently employed in industrial applications have achieved a photovoltaic conversion efficiency of more than 20% [3, 4]. However, such silicon-based solar cells are characterised by a high cost, harsh preparation conditions, and serious environmental pollution. Cadmium telluride and copper indium gallium selenium thin-film solar cells have achieved a high efficiency of photovoltaic conversion in the laboratory, but the industrial applications are restricted by the high production cost, environmental pollution, and other problems [5]. In recent years, dye-sensitized solar cells, as the representative of the third-generation solar cells, have achieved a photoelectric conversion efficiency of more than 13% in the laboratory and have developed rapidly due to their significant advantages, including low cost, simple process, and high efficiency [4]. However, dye-sensitized cells still have two disadvantages. Firstly, in order to ensure the full absorption of sunlight's energy, the absorbing layer is thick (>10 μm) because it is difficult to achieve complete light absorption using a thinner absorbing layer in the solid-state cells [6, 7]. Secondly, organic dyes cannot avoid the phenomenon of light bleaching. These

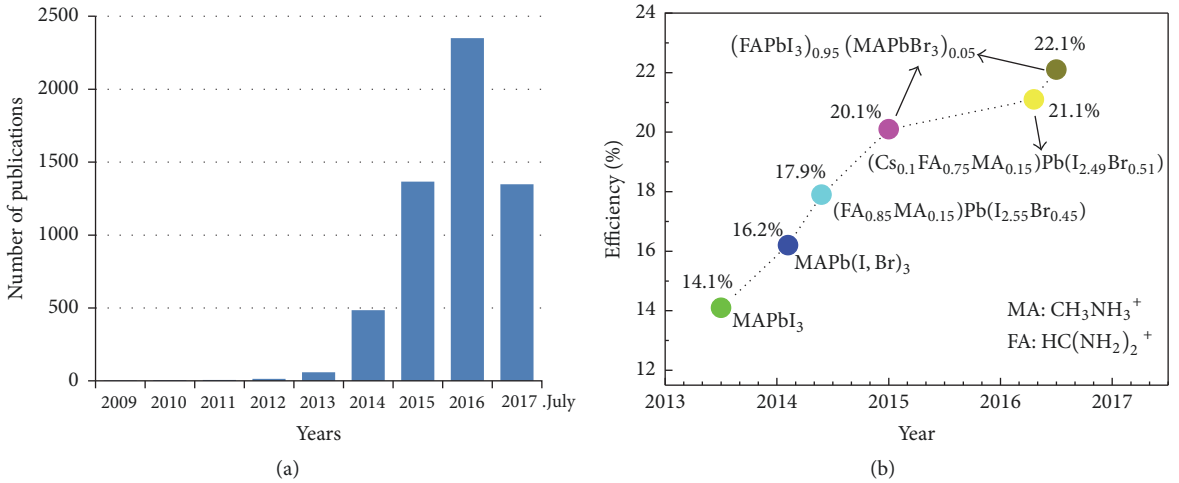

Figure 1: (a) Number of publications retrieved from Web of Science (Thomson Reuters) as a function of the year by the subject search "perovskite solar cells". (b) The best efficiencies of perovskite solar cells certified by the NREL.

two problems have prompted researchers to develop excellent all-solid dye materials.

In 2009, Japanese scientists Kojima et al. found that the organic metal halide perovskite was similar to dyes and can absorb sunlight. The perovskite can be applied in the dye-sensitized solar cells with a liquid electrolyte as a sensitizer to achieve power conversion efficiency (PCE) of 3.8% [8]. In 2012, Kim et al. reported all-solid-state perovskite solar cells with a PCE of 9.7% for the first time [9]. Because of the high efficiency and low cost, perovskite solar cells have attracted extensive attention from researchers worldwide and have developed rapidly in recent years. So far, the highest conversion efficiency has been 22.1% in 2016, which was certified by the National Renewable Energy Laboratory (NREL) [10, 11]. Further improvements in the performance of perovskite solar cells are expected to break the bottleneck of conversion efficiency and production cost. As one of the most promising novel photovoltaic cells, perovskite solar cells are of great scientific value and practical significance. Figure 1 shows the rapid increase in the number of publications regarding perovskite solar cells and the best efficiencies certified by the NREL.

This paper summarizes the advances in perovskite solar cells and details the structures and working principle of perovskite solar cells, the specific function and characteristics of each layer, and the preparation methods of perovskite light-absorbing layers. Finally, we outline the future research directions based on the reported results.

2. Structures and Working Principle of Perovskite Solar Cells

2.1. Perovskite Materials for Solar Cells. The perovskite material is derived from the calcium titanate ($CaTiO_3$) compound, which has the molecular structure of the type ABX_3. Perovskite materials have attracted wide attention because of the cubic lattice-nested octahedral layered structures and the unique optical, thermal, and electromagnetic properties.

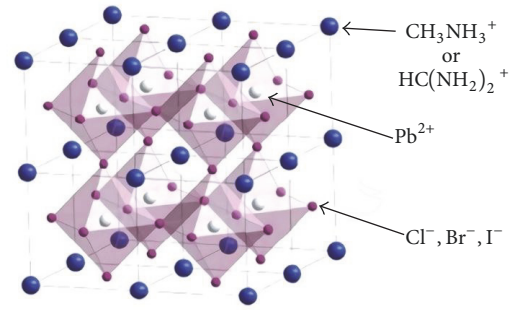

Figure 2: Typical perovskite cubic lattice structure. Reprinted from [12].

Perovskite materials used in solar cells are a kind of organic-inorganic metal halide compound with the perovskite structure, in which Group A (methylammonium, $CH_3NH_3^+$, MA^+, or formamidinium, $CH(NH_2)_2^+$, FA^+) is located in the vertex of the face-centred cubic lattice, and the metal cation B (Pb^{2+}, Sn^{2+}, etc.) and halogen anion X (Cl^-, Br^-, or I^-, or a coexistence of several halogens) occupy the core and apex of the octahedra, respectively. The metal-halogen octahedra are joined together to form a stable three-dimensional network structure. The crystal structure is shown in Figure 2.

The materials with such a structure have the following four features. Firstly, the materials possess excellent photoelectric properties, lower exciton binding energy, and high optical absorption coefficients (up to 10^4 cm^{-1}) [13]. Secondly, perovskite as the light-absorbing layer can absorb solar energy efficiently [14]. Thirdly, the materials possess a large dielectric constant and electrons and holes can be effectively transmitted and collected [15]. Lastly, electrons and holes can be transmitted simultaneously and the transmission distance is up to 100 nm or more and even more than 1 μm [16–19].

These features lead to a high open-circuit voltage (V_{oc}) and a short-circuit current density (J_{sc}) if the materials are employed in solar cell devices. During exposure to sunlight,

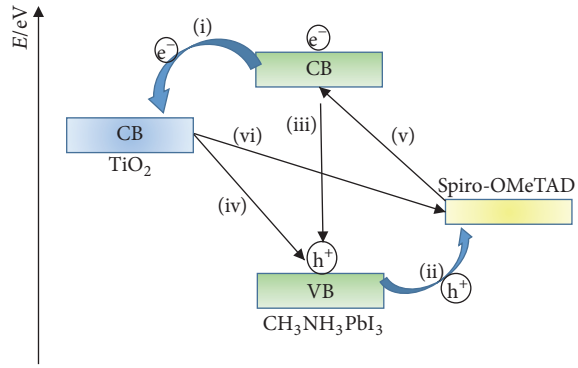

FIGURE 3: Schematic diagram of energy levels and transport processes of electrons and holes in a HTM/perovskite/TiO_2 cell.

the perovskite layer firstly absorbs photons to produce excitons (electron-hole pairs). Due to the difference in the exciton binding energy of the perovskite materials, these excitons can form free carriers (free electrons and holes) to generate a current or can recombine into excitons. Due to the low carrier recombination probabilities of $CH_3NH_3PbI_3$ ($MAPbI_3$) and other perovskite materials and the higher carrier mobility, the diffusion distance and lifetime of the carrier are long. For example, the carrier diffusion distance is at least 100 nm for $MAPbI_3$ and longer than 1 μm for $MAPbI_{3-x}Cl_x$ [16, 17]. The longer diffusion distance and lifetime of carriers are the source of the superior performance of perovskite solar cells. Then, these free electrons and holes are collected by an electron transport material (ETM) and a hole transport material (HTM). Electrons are transferred from the perovskite material to TiO_2, which is used for the ETM layers and finally collected by FTO. At the same time, the holes are transferred to the HTM layer and collected by the metal electrode. Finally, the FTO and metal electrode are connected and the photocurrent is generated in the outer circuit.

Marchioro et al. believed that the electron-hole pairs separated at the two heterojunction interfaces of TiO_2/perovskite and Spiro-OMeTAD/perovskite, followed by electrons injecting into TiO_2 (process (i) in Figure 3) and holes injecting into HTM (process (ii)) to achieve charges transport [20]. At the same time, a series of behaviours that are detrimental to the cell's performance, such as exciton annihilation (process (iii)), photoluminescence, or nonradiative recombination, as well as reverse transmission of electrons and holes (process (iv) and (v)) and recombination at the TiO_2/HTM interface (process (vi)) will also occur. The transport processes of electrons and holes in a HTM/perovskite/TiO_2 cell are shown in Figure 3.

In recent years, various structures of perovskite solar cells have been developed, including the mesoporous structure and the planar heterostructure. Figure 4 shows the structures of two typical perovskite solar cells: the mesoscopic architecture and the planar heterojunction structure. The characteristics and research progress of these two kinds of cell structures are described below.

2.2. Mesoporous Structure. Mesoporous materials have been extensively studied and widely applied because of their high porosity and large specific surface area (up to 1000 m^2/g). The application of mesoporous materials in perovskite solar cells allows the perovskite absorber to adhere to the mesoporous metal oxide framework for the purposes of increasing the light-receiving area of the photosensitive material and improving the efficiency of the device. As shown in Figure 4(a), a typical mesoporous solar cell consists of a FTO electrode, a dense electron transport layer, a mesoporous oxide layer, a perovskite layer, a hole transport layer, and an electrode layer. TiO_2 is the most typical mesoporous framework material, which allows the perovskite nanocrystals to penetrate into the pores of mesoporous TiO_2 by solution spin-coating and forms an interconnected absorbing layer. In this structure, TiO_2 not only plays a supporting role but also has significant functional roles, such as transporting electrons, blocking holes, and inhibiting the recombination of the electron-hole pairs in the FTO conductive substrate, which contributes to improving the photoelectric conversion efficiency of the device. In addition to TiO_2, the commonly used frame materials include mesoscopic metal oxides, such as ZnO, Al_2O_3, and ZrO_2. The hole transport layer is used to receive holes generated in the perovskite absorbing layer and transport them to the surface of the metal electrode. The most commonly used hole transport material is Spiro-OMeTAD (2,2′,7,7′-Tetrakis[N,N-di(4-methoxyphenyl)amino]-9,9′-spirobifluorene). Commonly used counterelectrode materials are noble metals, such as Au, Ag, and Pt. This kind of structure can not only effectively reduce the recombination probability of electrons and holes but also provide the required diffusion length for the effective collection of electrons and holes [21].

Kim et al. and Burschka et al. reported the all-solid-state $MAPbI_3$ solar cells based on the mesoscopic structure of porous nano-TiO_2. The filling factors (FF) were 0.62 and 0.73 and the PCEs were 9.7% and 15.0%, respectively [9, 22]. The significant improvement is mainly attributable to the high-quality perovskite films prepared by the two-step solution-deposition method. Burschka et al. believed that the conversion occurs within the nanoporous host as soon as the two components (MAI and PbI_2) come into contact, permitting much better control over the perovskite morphology [22]. Yang et al. reported a PCE greater than 20% at the end of 2014 using mesoscopic TiO_2/$FAPbI_3$ perovskite solar cell architecture [10]. Qiu et al. fabricated all-solid-state perovskite solar cells based on a one-dimensional TiO_2 nanoarray mesoscopic structure with $MAPbI_2Br$ as the light-absorbing layer and obtained a V_{oc} of 0.82 V and a PCE of 4.87% [23]. Qiu et al. showed that the PCEs initially increased and then decreased with the increasing length of the one-dimensional TiO_2 nanowire, thus verifying a balance between electron transport and perovskite loading. The perovskite solar cells based on mesoscopic TiO_2 involve high-temperature sintering and thus many scholars have studied the framework of perovskite cells utilising Al_2O_3 as the mesoscopic material.

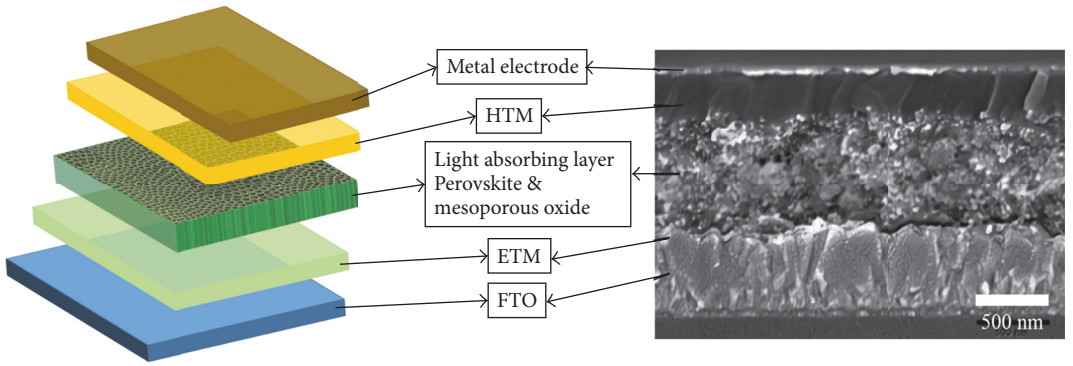

(a)

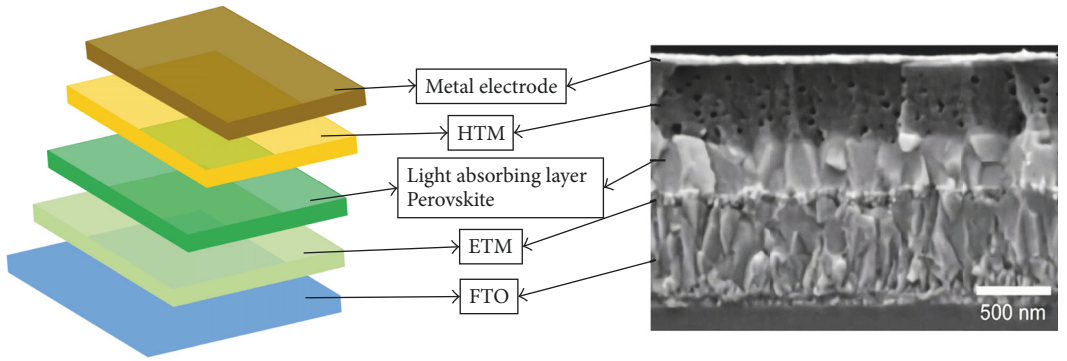

(b)

Figure 4: Schematic diagram and SEM section image of (a) mesoscopic architecture PSCs and (b) planar heterojunction structure PSCs.

Unlike TiO_2, Al_2O_3 acts only as a support layer in the device and does not play similar functional roles as that of TiO_2 for photoanode electron transport. Therefore, the connection between the Al_2O_3 particles becomes less important, thereby avoiding high-temperature sintering. The electrons generated in perovskite light-absorbing materials by light irradiation are not injected into the conduction band of Al_2O_3 but directly transported from the perovskite itself to the FTO conductive layer. In 2012, Lee et al.'s group prepared $MAPbI_3$ perovskite solar cells with Al_2O_3 as the support material to obtain a V_{oc} of 980 mV, a FF of 0.63, and a PCE of 10.9% [24]. After optimizing the process conditions, the conversion efficiency of the device increased to 12.3% [25]. In order to further improve the PCE of the devices utilising Al_2O_3, the Au@SiO_2 nanoparticles with a core-shell structure were doped into the Al_2O_3 layer to reduce the exciton binding energy, thus increasing the photoelectric conversion efficiency to 11.4% [26]. Like Al_2O_3, ZrO_2, and SiO_2 can also be used as the insulating support layer. The solar cells using $MAPbI_3$ loaded with ZrO_2 nanoparticles have V_{oc} of 1070 mV and a PCE of 10.8% [27]. Hwang et al. compared a series of perovskite solar cells with differently sized SiO_2 nanoparticles (15–100 nm) as the support layer and revealed that when the size of SiO_2 nanoparticles was 50 nm, the PCE was 11.45%, which was slightly higher than the PCE (10.29%) of the devices with the same-sized TiO_2 nanoparticles [28].

2.3. Plane Heterostructures. The typical planar heterojunction structure of the perovskite solar cells is shown in Figure 4(b). The main difference from the mesoscopic structure is that the planar structure removes the porous metal oxide framework. Two interfaces are formed between the perovskite materials and the two layers (the electron transport layer and the hole transport layer). Therefore, the electron-hole pairs are separated rapidly and effectively by the electron transport layer and hole transport layer, respectively. The studies on perovskite solar cells with a planar heterojunction structure contribute to the understanding of the mechanisms of light absorption and electron-hole separation and enhance the flexibility of device optimization for the development of highly efficient laminated perovskite solar cells. Snaith's group reported a FTO/TiO_2/$MAPbI_2Cl$/spiro-OMeTAD/Ag planar heterojunction structure of perovskite solar cells and reached a PCE of 1.8% [23]. Thereafter, the group prepared a series of solar cells with the planar structure, which achieved a maximum PCE of 15.7%, a V_{oc} of 1.03 V and a FF of 0.749 under optimized process conditions [29, 30].

Zhou et al. realized higher electron mobility by using yttrium-doped TiO_2 as the electron transport material and modified the ITO to reduce the working function, which is favoured to inject the electrons from TiO_2 to the ITO electrode. The open-circuit voltage and short-circuit current of the device were greatly improved and the PCE was as high as 19.3% [31]. Malinkiewicz et al. prepared $MAPbI_3$ perovskite solar cells by using poly(3,4-ethylenedioxythiophene): polystyrene sulfonate (PEDOT:PSS) to replace the conventional dense TiO_2 film and achieved a PCE of 12% [32]. This kind of structure is an inverted planar heterostructure

and has the potential for preparing flexible perovskite solar cells.

3. Advances in Perovskite Solar Cells

3.1. Perovskite Light-Absorbing Layer. Among all the components of perovskite solar cells, the perovskite materials play a core role in light absorption and photoelectric conversion. Perovskite compositions with single ions occupying each of the A-, B- and X-sites (e.g., $MAPbI_3$ and $FAPbI_3$) are denoted as "simple perovskites" and have been intensively studied. In fact, as shown in Figure 1(b), following pure $MAPbI_3$, the subsequent five NREL records with publicly disclosed information used A- and/or X-site mixed hybrid perovskites. The optimization of materials and structures is one of the keys to improving the photoelectric conversion efficiency. Table 1 shows some representative devices and their architectures and performance.

3.1.1. Mixed X Halide Anions. It has been reported that the electronic structure of perovskite $MAPbX_3$ is related to the *p* orbit of X and Pb. The band gap of $MAPbX_3$ can be controlled by adjusting the *p* orbit of mixed X halide anions so as to absorb visible light under solar radiation [56–58]. The photovoltaic properties of mixed $MAPbI_{3-x}Br_x$ were first demonstrated by Noh et al. and the efficiency reached 12.3% [59]. In the work by Noh et al., a lower Br content (<10%) yielded the highest initial efficiency due to the narrow band gap, but the higher Br content (>20%) achieved a good high-humidity shelf-life stability (RH 55% for 20 days). Noh et al. believed that the good stability is closely correlated to the transformation from a tetragonal phase to a pseudocubic phase due to the incorporation of the smaller ionic radius of Br^- and, consequently, led to a more compact and tightly bound structure with a higher tolerance factor. The close accumulation of perovskite structure, to a certain extent, prevented the degradation of $CH_3NH_3^+$ [59]. Jeon et al. achieved a best PCE of 18.4% in perovskite solar cells using $(FAPbI_3)_{1-x}(MAPbBr_3)_x$ (x = 0–0.3) as a light-absorbing layer through the solvent engineering method, which allowed the deposition of uniform and dense perovskite films [50].

By combining first-principles total-energy calculations with statistical mechanical treatments, Brivio et al. reported the two most stable configurations corresponding to ordered structures of $MAPbIBr_2$ and $MAPbI_{1/2}Br_{5/2}$. Both structures are layered superlattices along the [001] direction. The halogen ions locate at the corners of Pb-X octahedron, and the iodine ions locate at the top and/or bottom sites of each octahedron. These two ordered structures provide the structural freedom to separate the Pb-I (longer) and Pb-Br (shorter) interatomic separation along distinct directions, so that the internal strain is minimized and the architecture is most stable [60].

$MAPbI_{3-x}Cl_x$ is a perovskite structure formed by doping Cl atoms with partially substituted I atoms and it is one of the most extensively studied binary mixed perovskites. In 2013, Stranks et al. indicated that the diffusion length of electrons and holes in $MAPbI_{3-x}Cl_x$ was greater than 1 μm and that Cl doping improved the stability and conductivity of perovskite materials [61, 62]. Docampo et al. prepared $MAPbI_{3-x}Cl_x$ films using a two-step dipping method for application in perovskite solar cells and achieved a light current density of 22 mA cm^{-2} and a PCE of 15.41% [63]. The lifetime for photo-induced electrons reached 300 ns and the initial absorption edge for light absorption was improved. Based on the first-principles calculation, Mosconi et al. reported that the aggregation of Cl ions at the perovskite/ETM interface enhanced the binding energy between the $MAPbI_{3-x}Cl_x$ (110) crystal surface and the TiO_2 interface. Furthermore, the contact between the $MAPbI_{3-x}Cl_x$ perovskite and the TiO_2 adjusted the electronic structure of the interface and an electron tunnelling effect was generated, thus improving the stability in air and the conductivity for perovskite materials [64].

As a more complex ternary halide, the triple-halide-mixed $MAPb(I/Br/Cl)_3$ system has seldom been reported. Similar to that discussed above, Cl also affected the device performance by improving the carrier absorptivity. Meanwhile, Br was observed to strongly influence the band gap of the $MAPb(I/Br/Cl)_3$ system and, consequently, increased the open-circuit voltage [65]. In addition, Br incorporation was reported to stabilize the crystal lattice thus improving the lifetime of the device [66]. Chiang et al. synthesized high-quality $MAPb(I/Br/Cl)_3$ perovskite film by a combined hot-solution spin-coating and solvent annealing method. The inverted solar cell devices ($ITO/PEDOT:PSS/MAPbI_{3-x-y}Br_xCl_y/PC61BM/Ca/Al$) achieved J_{sc} of 19.25 mA/cm^2, V_{oc} of 1.10 V, FF of 78%, and PCE of 16.52% [67].

3.1.2. Mixed A-Site Cations. In the cubic perovskite structure, it is generally believed that the energy band structure of perovskite can be adjusted within a certain range by changing the size of the A-site ions. A larger (e.g., FA^+ = 0.19–0.22 nm) or smaller (e.g., Cs^+ = 0.167 nm, Rb^+ = 0.152 nm) cation causes the lattice to expand or contract, thus changing the B-X bond length, which has been shown to influence the band gap [68, 69]. Pellet et al. reported the first mixed A-cation and described the band gap tunability of $(MA)_x(FA)_{1-x}PbI_3$-based solar cells by varying the ratio of MA^+ to FA^+ and showed that the composition of $(MA)_{0.6}(FA)_{0.4}PbI_3$ resulted in the highest PCE of 14.52% with the absorption edge extending to ~810 nm [70]. Lee et al. prepared $FAPbI_3/MAPbI_3$ films with stacked structures by ion exchange, extended the absorption range of the long-wave spectrum, and reported a current density of 20.22 mA cm^{-2} and the best PCE of 16.01% [44]. Among the optimized MA^+/FA^+ ratios, it was found that $(MA)_{0.6}(FA)_{0.4}PbI_3$ resulted in the highest PCE of 18.3% [71].

It is known that inorganic materials usually exhibit higher stability than organic materials. Therefore, the design of replacing the organic cations with inorganic monovalent cations in the perovskite structure was put forward. Choi et al. devised $Cs_x(MA)_{1-x}PbI_3$ perovskite solar cell devices with x = 0.1 (inverted structure: ITO/PEDOT:PSS/$Cs_{0.1}(MA)_{0.9}PbI_3$/PCBM/Al) and achieved a PCE of 7.68% [72]. Niu et al. reported a higher efficiency of 18.1% in their

Table 1: Some representative devices, architectures, and their parameters and efficiencies (c-TiO_2 and mp-TiO_2 represent compact and mesoporous TiO_2, resp.).

Device architecture	HTM	J_{sc} ($mA \cdot cm^{-2}$)	V_{oc}/V	FF	η/%	Ref.
Based on $MAPbI_3$						
FTO/TiO_2/$MAPbI_3$/HTM/Au (one-step solution method)	Spiro-OMeTAD	18.94	1.07	0.65	13.23	[33]
FTO/TiO_2/$MAPbI_3$/HTM/Au (two-step solution method)	Spiro-OMeTAD	21.52	1.04	0.672	15.08	[34]
FTO/c-TiO_2/$MAPbI_3$/HTM/Ag	Spiro-OMeTAD	19.8	0.924	0.663	12.1	[35]
FTO/TiO_2/$MAPbI_3$/HTM/Au	MeO-PheDOT	18.31	0.914	0.636	10.64	[36]
FTO/mp-TiO_2/$MAPbI_3$/HTM/Au	P3HT	12.6	0.73	0.732	6.7	[37]
FTO/HTM/$MAPbI_3$/PCBM/Ag	$Cu_yCr_zO_2$	17.19~20.08	1.00~1.07	0.68~0.7	12.24~15.30	[38]
FTO/HTM/$MAPbI_3$/PCBM/Ag	Cu:CrOx	16.02	0.98	0.7	10.99	[39]
FTO/TiO_2/$MAPbI_3$/HTM/Au	Cu_2ZnSnS_4	20.54	1.06	0.587	12.75	[33]
FTO/TiO_2/$MAPbI_3$/HTM/Au	$Cu(In,Ga)(S,Se)_2$	17.66	0.94	0.549	9.15	[34]
FTO/TiO_2/$MAPbI_3$/Au	None	17.8	0.905	0.65	10.49	[40]
Perovskites based on mixed X halide						
FTO/TiO_2/$MAPbI_{3-x}Cl_x$/HTM/Au	Spiro-OMeTAD	21.45	1.08	0.74	17.14	[41]
ITO/Y-TiO_2/$MAPbI_{3-x}Cl_x$/HTM/Au	Spiro-OMeTAD	22.75	1.13	0.75	19.3	[31]
FTO/c-TiO_2/$MAPbI_{3-x}Cl_x$/HTM/Ag	Spiro-OMeTAD	21.5	1.07	0.67	15.4	[30]
ITO/HTM/$MAPbI_{3-x}Cl_x$/C60/Bphen/Ca/Ag	PEDOT:PSS	20.9	1.02	0.722	15.4	[42]
FTO/TiO_2/$MAPbI_{3-x}Cl_x$/HTM/Au	$CuGaO_2$	21.66	1.11	0.77	18.51	[41]
FTO/c-TiO2/mp-TiO_2/$MAPbI_{3-x}Br_x$/HTM/Au	PTAA	19.5	1.09	0.76	16.2	[43]
Perovskites based on mixed A-site cations						
FTO/c-TiO_2/$FAPbI_3$/$MAPbI_3$/HTM/Au	Spiro-OMeTAD	20.97	1.032	0.74	16.01	[44]
ITO/HTM/$FA_{0.4}MA_{0.6}PbI_3$/C60/Cu	PTAA	23.0	1.03	0.77	18.3	[45]
FTO/TiO_2/$FA_{0.8}MA_{0.1}Cs_{0.1}$/HTM/Au	Spiro-OMeTAD	21.5	1.155	0.73	18.1	[46]
FTO/SnO_2/$FA_{0.8}MA_{0.1}Cs_{0.1}$/HTM/Au	Spiro-OMeTAD	22.4	1.129	0.68	17.3	[46]
FTO/TiO_2/ZrO_2/$(5\text{-AVA})_x(MA)_{1-x}PbI_3$/Carbon (certificated by an accredited photovoltaic calibration laboratory)	None	22.8	0.858	0.66	12.84	[47]
FTO/TiO_2/ZrO_2/$(5\text{-AVA})_x(MA)_{1-x}PbI_3$/Carbon (perovskite film with larger grain size of 30 μm)	None	22.57	0.801	0.62	11.35	[48]
Perovskites based on mixed A- and X-site ions						
FTO/c-TiO_2/mp-TiO_2/$(SrCl_2)_{0.1}$:$MAPbI_3$/Carbon	None	20.18	1.05	0.75	15.9	[49]
FTO/TiO_2/$(FAPbI_3)_{0.85}(MAPbBr_3)_{0.15}$/HTM/Carbon	PEDOT	23.5	1.05	0.69	17.0	[45]
FTO/c-TiO_2/mp-TiO_2/$(FAPbI_3)_{0.85}(MAPbBr_3)_{0.15}$/HTM/Au	PTAA	22.5	1.11	0.73	18.4	[50]
All-inorganic metal halide perovskites						
FTO/c-TiO_2/mp-TiO_2/$CsPbBr_3$/Carbon	None	7.4	1.24	0.73	6.7	[51]
FTO/c-TiO_2/$CsPbI_3$ QDs/HTM/MoO_x/Al	Spiro-OMeTAD	13.47	1.23	0.65	10.77	[52]
FTO/c-TiO_2/mp-TiO_2/$CsPbIBr_2$/HTM/Au	Spiro-OMeTAD	7.8	1.13	0.72	6.3	[53]
ITO/c-TiO_2/$CsPbI_2Br$/HTM/Ag	Spiro-OMeTAD	13.99	1.10	0.67	10.34	[54]
FTO/c-TiO_2/$Cs_{0.925}K_{0.075}PbI_2Br$/HTM/Au	Spiro-OMeTAD	11.6	1.18	0.73	10.0	[55]

optimized $Cs_x(MA)_{1-x}PbI_3$ cell device with $x = 0.09$ (regular structure: FTO/c-TiO_2/mp-TiO_2/$Cs_{0.09}(MA)_{0.91}PbI_3$/Spiro-OMeTAD/Au). In addition, the thermal stability (aging temperature of 85°C) of the unencapsulated devices was significantly improved compared to $MAPbI_3$ [73]. Recently, the Rb^+ cation, which has an even smaller ionic radius (0.152 nm) than Cs^+ (0.181 nm), has also received wide attention because it can further enhance both the efficiency and stability of Rb-mixed perovskite solar cells. Park et al. studied the (FA/Rb)PbI_3 system using the same Rb quantity ($x \leq 0.05$) and, respectively, achieved PCEs of 16.15% and 16.2% [74, 75]. More importantly, the significantly enhanced stability against moisture at 85% RH of Rb-mixed perovskites was highlighted.

In order to further improved the stability of the perovskite solar cells, introducing all-inorganic perovskites into photovoltaic devices was proposed, owing to their superior stability, especially at high temperature. Swarnkar et al. prepared stable $CsPbI_3$ quantum dots and films, which exhibited good stability when exposed the films into the ambient atmosphere for 60 days and showed a PCE up to 10.77% and a V_{oc} of 1.23 V in perovskite solar cells [52]. Kulbak et al. reported $CsPbBr_3$ perovskite solar cells with a PCE of 5.95% and compared the thermal stability of the $CsPbBr_3$ and $MAPbBr_3$, confirming that the $CsPbBr_3$ can endure much higher temperature of up to 580°C and displayed a higher stability during two weeks [76]. Although the works mentioned above displayed the high stability for solar devices, the structures still contained organic HTM. Jin et al. reported the design of all-inorganic perovskite solar cell devices, in which the organic HTM and metal electrode were completely eliminated and a layer of carbon electrode was coated on the $CsPbBr_3$ layer [51]. The entire fabrication process of the all-inorganic PSCs can be operated in ambient environment without humidity control. The PSCs presented a PCE of 6.7% when it was illuminated and showed no performance degradation even in humid air (90–95%, RH, 25°C) without encapsulation for over 3 months. Combining the good stability of $CsPbBr_3$ and the small band gap of $CsPbI_3$, the halide mixed all-inorganic perovskites of $CsPb(I_{1-x}Br_x)_3$ were proposed [53, 54, 77, 78]. In addition, Nam et al. incorporated potassium cations into the $CsPbI_2Br$ and reported that the $Cs_{0.925}K_{0.075}PbI_2Br$ based perovskite solar cells exhibited the maximum and average PCEs of 10.0 and 9.1% and displayed higher stability than those based on $CsPbI_2Br$ [55]. The results suggest that the stability of all-inorganic perovskites can be further improved by incorporating some specific cations into the unit cells, such as Ag^+ and Bi^{3+}.

3.1.3. Mixed B-Site Cations. The toxicity of Pb restricts its large-scale application. Therefore, lead-free perovskite materials have been explored. Sn and Pb belong to the same family in the periodic table of chemical elements and, therefore, Sn has become the primary alternative to Pb. In general, the band gap of perovskite materials based on Sn^{2+} is less than those based on Pb^{2+} and, therefore, it can be used to prepare perovskite materials with mixed Sn and Pb in the B-site so that the absorption can reach the near-infrared region. Ogomi et al. studied the optical properties of $MASn_{1-x}Pb_xI_3$ with different ratios of Pb to Sn and found that the band gap could be adjusted within the range 1.17–1.55 eV and that the optical absorption wavelength could be extended to 1060 nm [79]. However, due to the narrow band gap, the open-circuit voltage of the device decreased. In addition, since Sn^{2+} is easily oxidized to Sn^{4+}, the self-doping of Sn^{4+} affects the stability of the perovskite films, thus resulting in instability and lower power conversion efficiency of the solar cells. Sn-based perovskite solar cells have been reported to demonstrate PCEs of around 5-6% in the conventional plane structures [80–83]. Zou et al. reported the synthesis of binary Pb-Sn perovskites ($MAPb_{1-x}Sn_xI_{1-y}Cl_y$) and achieved a PEC of 10.1% in an inverted planar heterojunction device [82]. Recently, Liu et al. reported C60-modified Sn-Pb perovskite films ($MAPb_{1-x}Sn_xI_3$) and achieved an impressive PEC of 13.9% (with $x = 0.25$) in an inverted planar heterojunction device. Importantly, the hybrid Sn-Pb perovskite solar cells modified with the C60 additive were demonstrated to have superior stability and efficiency when exposed to the ambient environment without encapsulation [84]. Marshall et al. described the inorganic perovskite materials of $CsSnI_3$ and indicated that the addition of $SnCl_2$ in the light-absorbing layer was the most significant for improving the stability and could not reduce the energy-conversion efficiency [85]. In addition, the studies on replacing Pb by Ge and/or Bi indicated that the low energy-conversion efficiency was ascribed to the solubility and carrier recombination of perovskite materials [86, 87].

3.1.4. Simultaneous Mixed A- and X-Site Ions. The more complex systems of simultaneously mixed A- and X-site perovskites have been extensively studied in recent years. As shown in Figure 1(b), out of six certified efficiencies reported by the NREL, three were based on the (FA/MA)Pb(I/Br) and (Cs/FA/MA)Pb(I/Br) perovskite systems. Zheng et al. reported that the (FA/MA)Pb(I/Br) system showed enhanced stability under storage conditions in air (~50% RH, 23°C) without encapsulation compared with $FAPbI_3$-based perovskite solar cells [88]. It was proposed that when MABr is incorporated into alloys with $FAPbI_3$, the lattice size is reduced, and the strain forces are relaxed. In this way, the pseudocubic α-phase is stabilized at room temperature and even in humid air. The studies on ternary and quaternary mixed cation systems of (Cs/FA/MA)Pb(I/Br) and (Rb/Cs/FA/MA)Pb(I/Br) generally focused on the design of multicomponent perovskites to achieve a stable, single, pure phase that can enable the creation of stable structures with optimal transport and even higher PCEs [46, 89, 90].

3.2. Electron Transport Layer. The basic function of the electron transport layer is to form an electron-selective contact with the perovskite light-absorbing layer to improve the extraction efficiency of photo-generated electrons and to effectively prevent the hole from migrating to the counterelectrode so as to enhance the carrier's separation effect and to reduce the recombination. At present, TiO_2, which has a wide band gap, has been widely studied as an effective electron transport material. In addition, ZnO and other

n-type semiconductor materials are often used as electron transport layers and are employed in flexible perovskite solar cells. Many studies on electron transport materials focus on the effects of different *n*-type semiconductor materials and structures on the power conversion efficiency [91–94]. The basis for the selection of electron transport materials is as follows. Firstly, the *n*-type semiconductors with the higher carrier mobility are recommended. Secondly, the material should be transparent to visible light due to a relatively wide band gap. Thirdly, the preparation conditions should be mild and the material can be obtained at low temperatures. Fourthly, the band structure should match the perovskite materials. In fact, the electron transport layer formed by different systems and structures can achieve high power conversion efficiency, indicating that the selection of commonly used electron transport materials is not the main factor that restricts the power conversion efficiency of solar cells [95].

In addition, an organic electron transport layer is being developed. Docampo et al. found that the ability of PCBM (one of the fullerene derivatives, [6, 6]-phenyl-C61-butyric acid methyl ester) and PFN (poly[9,9-dioctylfluorene-9,9-bis(N,N-dimethylpropyl)fluorene]) to collect electrons was better than that of inorganic TiO_2 in inverted solar cells. Perovskite solar cells were prepared with PCBM as the electron transport layer and PEDOT:PSS as the hole transport layer and such cells achieved a PCE of 9.8% [96].

3.3. Hole Transport Layer. The main role of the hole transport layer is to collect and transport holes from the perovskite light-absorbing layer to promote the separation of the electron-hole pairs in the perovskite materials through cooperating with the electron transport layer. In hole transport materials, the highest occupied molecular orbit (HOMO) must match the valence band of perovskite materials for hole transport. According to the chemical composition, hole transport materials in perovskite solar cells can be divided into two types: organic and inorganic hole transport materials. Spiro-OMeTAD is the most commonly used organic hole transport material, which shows good penetration in nanoscale perovskite and is a good match with the valence band energy of perovskite, although its hole mobility is not as high as that of other organic hole transport materials. Some scholars [97] doped a *p*-type composite (i.e., cobalt compounds) or some additives (i.e., bis(trifluoromethane) sulfonimide lithium, LiTFSI, and 4-tert-butyl pyridine, TBP) into organic materials to improve the hole mobility. Compared with the organic small-molecule materials, polymer hole transporting materials have attracted more and more attention due to their better film-forming ability and higher hole mobility. PTAA (poly[bis(4-phenyl)(2,4,6-trimethylphenyl)amine]) is commonly used as the hole transport material because its hole mobility is one to two orders of magnitude higher than that of other hole transport materials. Jeon et al. prepared $MAPbI_3$ perovskite solar cells using PTAA as the hole transport material and obtained the highest PCE of 16.2% and a short-circuit current of 21.3 mA cm^{-2} [98]. Other polymer hole transport materials include P3HT, PEDOT:PSS, PCDTBT, and PCPDTBT. Zhang et al. studied the role of P3HT in perovskite solar cells and indicated that the presence of P3HT can reduce the resistance from the hole transfer impedance and thus improve the stability and performance of the devices [99]. PEDOT:PSS is commonly used in photovoltaic devices with flexible substrates because it is easy to form films in solution [100].

Compared with organic hole transport materials, inorganic *p*-type semiconductor materials show the potential to replace organic hole transport materials due to their advantages, which include high hole mobility, wide band gap, and simple solvent treatment process. Many inorganic hole transport materials have been reported, such as CuI, NiO, $CsSnI_3$, and CuSCN. The conductivity of CuI is better than that of Spiro-OMeTAD and thus CuI effectively improves the filling factor of the device and is a powerful competitor to Spiro-OMeTAD [101]. Seo et al. prepared perovskite solar cells based on $MAPbI_3$ and achieved a PCE of 16.4% with an undoped NiO ultrathin film as the hole transport layer by atomic layer deposition [102]. The work function and the hole concentration increased remarkably due to the overlap of the Debye length in NiO ultrathin films. Qin et al. reported that the PCE of the device reached 12.4% and the short-circuit current was greatly increased with CuSCN as the hole transport material due to its higher hole mobility than that of Spiro-OMeTAD (0.01–0.1 cm^2/V·s for CuSCN and 4×10^{-5} cm^2/V·s for Spiro-OMeTAD) [103]. In addition, Zhang et al. reported a perovskite solar cell using nanoscale $CuGaO_2$ and achieved a PCE of 18.51%, which was one of the highest efficiencies among all perovskite solar cells using inorganic HTM. More importantly, it was found the employment of $CuGaO_2$ significantly improved the long-term stability of perovskite solar cells. The PCE of $CuGaO_2$-based device maintains the major performance up to 30d under ambient environment (30%–55% humidity, $T = 25^{\circ}C$) [41].

3.4. Solar Cells without the Hole Transport Layer. Recently, perovskite solar cells without the hole transport material have become an important research direction and such solar cells show great potential due to their advantages of simple structure, easy preparation process and high stability. In HTM-free perovskite solar cells, perovskite materials are used simultaneously as light absorbers and hole transport channels. The results obtained by Minemoto and Murata, who used a device simulation method, showed that the lack of hole transport layers did not affect the built-in electric field when the work function of metal electrodes was close to the maximum valence band of light-absorbing materials [104]. In contrast, the built-in electric field decreased rapidly when the work function was below the peak of the valence band, thus leading to a reduction of the device's open-circuit voltage and the photoelectric conversion efficiency. Therefore, the work function of the metal electrodes is an important factor in the HTM-free perovskite solar cells. Shi et al. assembled HTM-free FTO/TiO_2/$MAPbI_3$/Au solar cells with the best PCE of 10.49% and V_{oc} of 905 mV [40]. The Schottky contact between the perovskite semiconductor and the metal electrode was suppressed by introducing an ultrathin Al_2O_3 film between the perovskite and Au electrode, thus improving the performance of the devices [105]. In

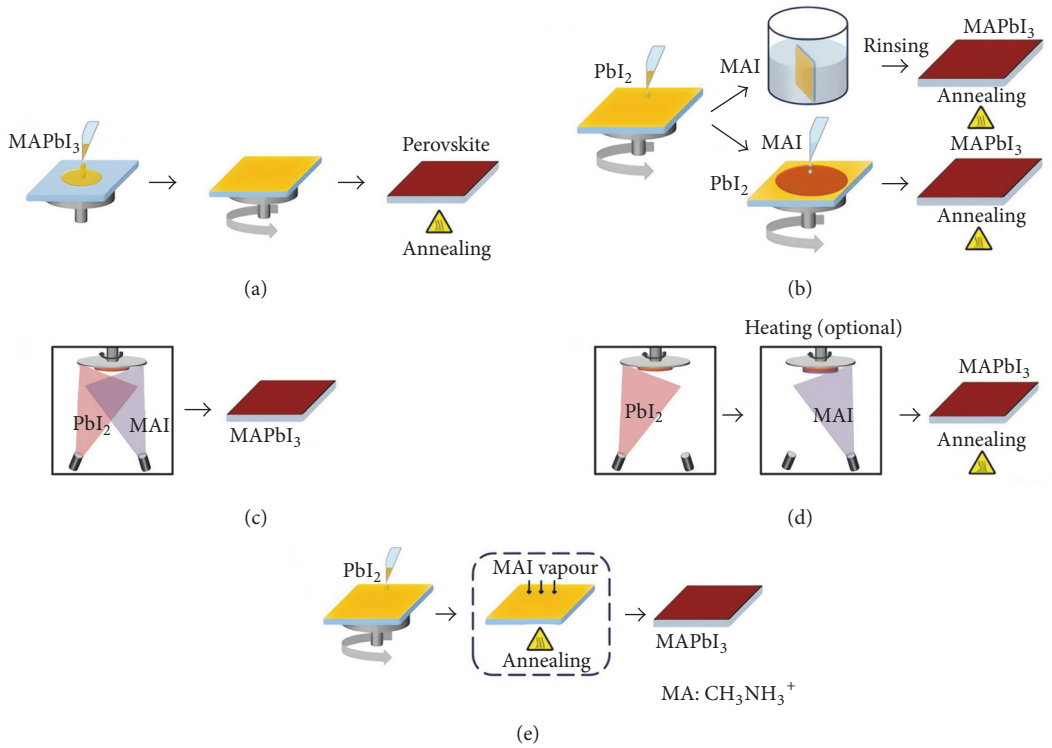

Figure 5: Illustration of different deposition methods for perovskite layer: (a) solution-based one-step method, (b) solution-based two-step method, (c) dual-source vapour-deposition method, (d) sequential vapour-deposition method, and (e) vapour-assisted solution method. Reprinted with permission from [107].

addition, the energy band mismatch between absorbers and electrodes could be significantly reduced by replacing the traditional Au electrode by back contact materials with a high work function. Subodh et al. prepared HTM-free solar cells by replacing the metal electrodes with laminated carbon nanotube networks as the hole-collecting layers and achieved a PCE of 6.87% [106]. The theoretical simulation results by Wang et al. showed that the appropriate thickness of the absorbing layer and *p*-type doping were beneficial to the efficiency of the HTM-free perovskite solar cells. According to Wang's theoretical calculation, the PEC of perovskite solar cells without the hole transmission layer is expected to exceed 17% after structural optimization [105].

4. Preparation Methods of the Perovskite Light-Absorbing Layer

The synthesis methods of the light-absorbing layer of perovskite solar cells can be roughly divided into three types: the solution method, the vapour-deposition method, and the vapour-assisted solution method. The solution method is simple and economical, but more internal defects will be produced in synthetic crystals and the hole transport layer is in direct contact with the electron transport layer, thus reducing the device's filling factor and the open-circuit voltage. The perovskite films prepared by the vapour-deposition method show a high surface density and fewer defects, which improve the filling factor and the open-circuit voltage. However, this method requires a high-vacuum environment and involves high energy consumption. The vapour-assisted solution method integrates the advantages of the solution method and the evaporation method. At a lower vacuum, the perovskite materials with fewer internal defects can be synthesized. Figure 5 illustrates the different deposition methods for perovskite layer. Table 2 shows a comparison of the common fabrication techniques of perovskite layer.

4.1. Solution Method. The solution synthesis methods of perovskite materials can be divided into one- and two-step methods according to the number of deposition steps. The one-step synthesis of the perovskite light-absorbing layer is described briefly below. PbX_2 and MAX are dissolved in solvents at a certain stoichiometric ratio to form a precursor solution, which is then directly spin-coated on a TiO_2 substrate and dried at a suitable temperature and atmosphere to obtain the light-absorbing perovskite layer. The crystal quality and properties of the perovskite layer are closely related to the solvent used, annealing temperature, and annealing time [94, 108]. The one-step deposition method is simple, but it is not easy to control the morphology and size of the synthetic crystals. A two-step sequential deposition method was first proposed by Liang et al. [109]. In this method, a saturated methanol solution of PbI_2 is used as the precursor solution for the spin-coating on the TiO_2 substrate. And then, the PbI_2-coated substrate is immersed in a 2-propanol solution containing MAI for suitable time and then rinsed with 2-propanol. After drying at a suitable temperature, the PbI_2 reacts with MAI and the perovskite layer is synthesized. The

Table 2: A comparison of the common fabrication techniques.

Method	Description	Advantages	Disadvantages
One-step solution deposition	A solution containing the organic and inorganic components is spin-coated on a substrate followed by annealing to form perovskite	Cost-effective, straightforward to implement	Poor film quality leads to limited efficiency, choice of a solvent that can simultaneously dissolve both components is limited
Two-step solution-based processing	A solution of the inorganic component is spin-coated on a substrate, subsequent spin-coating (or immersing) of a solution containing the organic component followed by annealing	Better photovoltaic performance compared to one-step methods	Less control over film thickness as compared to vacuum processes
Dual-source vapour deposition	The organic and inorganic components are coevaporated and then annealed to give perovskite	Better film uniformity, as compared to solution processes leading to better efficiencies	Vacuum process leads to high energy requirements, and it is difficult in simultaneously controlling the deposition rates of both components
Sequential vapour deposition	A bilayer film of the inorganic and organic components is prepared by sequential deposition, followed by thermal annealing to give perovskite	Eliminates problems of one-step codeposition	Vacuum process, which leads to high energy requirements, higher costs, limiting mass production
Vapour assisted solution process	First, an inorganic component is deposited by spin-coating and then is exposed to the vapour of the organic component at an elevated temperature	Combination of vapour and solution-based processes gives better film quality	Vacuum process leads to high energy requirements

dipping time and MAI solution concentration are crucial to the morphology and optoelectronic properties of the final $MAPbI_3$ films. Burschka et al. prepared perovskite solar cells with a high PCE of 15% according to a slightly modified two-step method by spin-coating MAI solution on the PbI_2 film rather than dipping [22]. Compared with the one-step solution method, the two-step method is beneficial to the fabrication of perovskite films under the relatively high humidity, where the relative humidity less than 60% was hard to affect the overall performance [110].

4.2. Vapour-Deposition Method. The vapour-deposition synthesis method of the perovskite absorbing layer is generally carried out under high-vacuum conditions. PbX_2 and MAX are deposited simultaneously or alternately on the precoated TiO_2 substrate by thermal evaporation from dual sources of PbX_2 and MAX. $MAPbX_3$ is formed at a suitable temperature and atmosphere and then crystallized into a perovskite film. Snaith et al. first reported the coevaporation deposited $MAPbI_3$ film and applied it in the planar heterojunction perovskite solar cells, achieving PCE of 15.7% and J_{sc} of $21.5\,mA{\cdot}cm^{-2}$ [6, 16, 30]. However, the method requires high temperature to evaporate the solid PbI_2 into vapor. The method has high requirements for equipment and may produce toxic gases. The drawbacks of the synthesis of the perovskite layer could be avoided if a new metal halide with low evaporation temperature and low toxicity can be developed and selected to replace PbI_2.

Similar to the two-step solution process, a modified vapour-deposition method, named "sequential vapour deposition," was proposed, in which PbX_2 was first deposited by thermal evaporation followed by vapour deposition of MAX. This sequential deposition was developed because of the difficulty in monitoring the MAI deposition rate in the codeposition process. The photovoltaic performance of the devices prepared by the sequential deposition was found to depend significantly on the substrate temperature. Chen et al. reported that the devices based on $MAPbI_3$ perovskite thin films prepared by the sequential vapour-deposition method exhibited a PCE of 15.4% [42]. Forgács et al. reported a perovskite/perovskite tandem solar cell fabricated by sequential vapour deposition and delivered a maximum PCE of 18%, thus highlighting the potential of sequentially deposited multilayer structures to improve the efficiency of single-junction perovskite devices [111].

4.3. Vapour-Assisted Solution Method. The vapour-assisted solution method is a relatively economical synthesis method of high-quality light-absorbing perovskite layers. It was developed to avoid the drawbacks of the solution method and the vapour-deposition method. The process of the vapour-assisted solution method can be outlined as below. PbX_2 is deposited on FTO glass covered with TiO_2 by the solution method and then $MAPbX_3$ grains grow by in situ reaction in MAX vapour at 120–165°C in a nitrogen atmosphere for 2–4 h. Chen et al. first reported perovskite films with microscale grain sizes, low surface roughness, and complete surface coverage by using the vapour-assisted solution method [112]. They applied the films in the planar heterojunction perovskite solar cells and measured an average PCE of 12.1% with high reproducibility. However, in the vapour-assisted solution method, the PbX_2 films at the bottom cannot react completely with the MAX vapour, thus increasing the internal resistance and decreasing the output power of the perovskite cells.

Among the above-mentioned preparation methods, the development of preparation methods aims to obtain compact perovskite films with high purity, few defects, and high coverage. The essential purpose of the research into these preparation methods is to improve the electrical contact between different layers, to reduce the defect density and the carrier loss during transmission, and to achieve a high power conversion efficiency.

5. Summary and Outlook

In this paper, we review the advances in the recent developments, as well as the fundamentals and basic structures of the perovskite solar cells. The versatility in the fabrication techniques of the perovskite light-absorbing layer, which include the solution-deposition method, vapour-deposition method, and the vapour-assisted solution method, is attractive and such methods are also discussed.

Perovskite solar cells have developed rapidly, but some critical factors may restrict the development of perovskite solar cells. Firstly, the stability of the organic lead halide perovskite is greatly affected by external environmental factors (such as humidity, temperature, and ultraviolet radiation), which lead to the low stability of the devices and the great difficulties in encapsulating cells in the later stage. Therefore, the development of a high-stability device composition, including the light-absorbing layer, electron/hole transport layer, and electrode materials, as well as the development of a simple and effective device-packaging method, will be of great significance to promote the practicability of such devices [113]. Secondly, the hole transporting material Spiro-OMeTAD used in perovskite solar cells is expensive (10 times the market price of gold) and its synthesis process is complex. Therefore, it is necessary to design and synthesize new hole transport materials to promote commercial applications of perovskite solar cells. Thirdly, it is difficult to deposit a large area of continuous perovskite film with the traditional methods described above and so other methods should be improved to prepare high-quality and large-area perovskite solar cells for commercial production in the future. Fourthly, the Pb element employed in perovskite solar cells is highly toxic, which will hinder the industrial promotion and development of perovskite solar cells. Therefore, it is necessary to find a low-toxicity or nontoxic ingredient to replace Pb in the future. Fifthly, there is a lack of deep understanding of the microscopic physics mechanism of perovskite solar cells. Therefore, it is necessary to establish a complete theoretical model to explain the reasons for the increase in the conversion efficiency. Theoretical studies will not only help to further improve the performance of perovskite solar cells but also provide ideas to develop simpler and/or more efficient new materials and structures. In a word, all the above issues need to be addressed

before making full application of the perovskite solar cells technology.

Conflicts of Interest

The authors declare no competing financial interests.

Acknowledgments

The authors would like to acknowledge the National Natural Science Foundation of China (Grants nos. 51502114 and 61405076).

References

[1] M. A. Green, S. R. Wenham, J. Zhao, J. Zolper, and A. W. Blakers, "Recent improvements in silicon solar cell and module efficiency," in *Proceedings of the Twenty First IEEE Photovoltaic Specialists Conference - 1990 Part 2 (of 2)*, pp. 207–210, May 1990.

[2] D. M. Chapin, C. S. Fuller, and G. L. Pearson, "A new silicon p-n junction photocell for converting solar radiation into electrical power," *Journal of Applied Physics*, vol. 25, no. 5, pp. 676-677, 1954.

[3] M. A. Green, K. Emery, Y. Hishikawa, W. Warta, and E. D. Dunlop, "Solar cell efficiency tables (version 41)," *Progress in Photovoltaics*, vol. 21, no. 1, pp. 1–11, 2013.

[4] S. Mathew, A. Yella, P. Gao et al., "Dye-sensitized solar cells with 13% efficiency achieved through the molecular engineering of porphyrin sensitizers," *Nature Chemistry*, vol. 6, no. 3, pp. 242–247, 2014.

[5] B. Parida, S. Iniyan, and R. Goic, "A review of solar photovoltaic technologies," *Renewable & Sustainable Energy Reviews*, vol. 15, no. 3, pp. 1625–1636, 2011.

[6] H. J. Snaith, "Perovskites: the emergence of a new era for low-cost, high-efficiency solar cells," *The Journal of Physical Chemistry Letters*, vol. 4, no. 21, pp. 3623–3630, 2013.

[7] A. Kojima, K. Teshima, T. Miyasaka et al., "Novel Photoelectrochemical cell with mesoscopic electrodes sensitized by lead-halide compounds (2)," *Meeting Abstracts: The Electrochemical Society*, p. 397, 2006.

[8] A. Kojima, K. Teshima, Y. Shirai, and T. Miyasaka, "Organometal halide perovskites as visible-light sensitizers for photovoltaic cells," *Journal of the American Chemical Society*, vol. 131, no. 17, pp. 6050-6051, 2009.

[9] H.-S. Kim, C.-R. Lee, J.-H. Im et al., "Lead iodide perovskite sensitized all-solid-state submicron thin film mesoscopic solar cell with efficiency exceeding 9%," *Scientific Reports*, vol. 2, article 591, 2012.

[10] W. S. Yang, J. H. Noh, N. J. Jeon et al., "High-performance photovoltaic perovskite layers fabricated through intramolecular exchange," *Science*, vol. 348, no. 6240, pp. 1234–1237, 2015.

[11] X. Li, D. Bi, C. Yi et al., "A vacuum flash-assisted solution process for high-efficiency large-area perovskite solar cells," *Science*, vol. 353, no. 6294, pp. 58–62, 2016.

[12] Z. Chen, H. Li, Y. Tang, X. Huang, D. Ho, and C.-S. Lee, "Erratum: Shape-controlled synthesis of organolead halide perovskite nanocrystals and their tunable optical absorption ((2014) Materials Research Express 1 (015034))," *Materials Research Express*, vol. 1, no. 3, Article ID 039501, 2014.

[13] S. Sun, T. Salim, N. Mathews et al., "The origin of high efficiency in low-temperature solution-processable bilayer organometal halide hybrid solar cells," *Energy Environ. Sci.*, vol. 7, no. 1, pp. 399–407, 2014.

[14] C. C. Stoumpos, C. D. Malliakas, and M. G. Kanatzidis, "Semiconducting tin and lead iodide perovskites with organic cations: phase transitions, high mobilities, and near-infrared photoluminescent properties," *Inorganic Chemistry*, vol. 52, no. 15, pp. 9019–9038, 2013.

[15] T. Baikie, Y. Fang, J. M. Kadro et al., "Synthesis and crystal chemistry of the hybrid perovskite $(CH_3NH_3)PbI_3$ for solid-state sensitised solar cell applications," *Journal of Materials Chemistry A*, vol. 1, no. 18, pp. 5628–5641, 2013.

[16] M. A. Green, A. Ho-Baillie, and H. J. Snaith, "The emergence of perovskite solar cells," *Nature Photonics*, vol. 8, no. 7, pp. 506–514, 2014.

[17] S. P. Singh and P. Nagarjuna, "Organometal halide perovskites as useful materials in sensitized solar cells," *Dalton Transactions*, vol. 43, no. 14, pp. 5247–5251, 2014.

[18] M. Luan, J. Song, X. Wei, F. Chen, and J. Liu, "Controllable growth of bulk cubic-phase CH3NH3PbI3 single crystal with exciting room-temperature stability," *CrystEngComm*, vol. 18, no. 28, pp. 5257–5261, 2016.

[19] I. Chung, B. Lee, J. He, R. P. H. Chang, and M. G. Kanatzidis, "All-solid-state dye-sensitized solar cells with high efficiency," *Nature*, vol. 485, no. 7399, pp. 486–489, 2012.

[20] A. Marchioro, J. Teuscher, D. Friedrich et al., "Unravelling the mechanism of photoinduced charge transfer processes in lead iodide perovskite solar cells," *Nature Photonics*, vol. 8, no. 3, pp. 250–255, 2014.

[21] E. Edri, S. Kirmayer, D. Cahen, and G. Hodes, "High open-circuit voltage solar cells based on organic-inorganic lead bromide perovskite," *The Journal of Physical Chemistry Letters*, vol. 4, no. 6, pp. 897–902, 2013.

[22] J. Burschka, N. Pellet, S. Moon et al., "Sequential deposition as a route to high-performance perovskite-sensitized solar cells," *Nature*, vol. 499, no. 7458, pp. 316–319, 2013.

[23] J. Qiu, Y. Qiu, K. Yan et al., "All-solid-state hybrid solar cells based on a new organometal halide perovskite sensitizer and one-dimensional TiO_2 nanowire arrays," *Nanoscale*, vol. 5, no. 8, pp. 3245–3248, 2013.

[24] M. M. Lee, J. Teuscher, T. Miyasaka, T. N. Murakami, and H. J. Snaith, "Efficient hybrid solar cells based on meso-superstructured organometal halide perovskites," *Science*, vol. 338, no. 6107, pp. 643–647, 2012.

[25] J. M. Ball, M. M. Lee, A. Hey, and H. J. Snaith, "Low-temperature processed meso-superstructured to thin-film perovskite solar cells," *Energy & Environmental Science*, vol. 6, no. 6, pp. 1739–1743, 2013.

[26] W. Zhang, M. Saliba, S. D. Stranks et al., "Enhancement of perovskite-based solar cells employing core-shell metal nanoparticles," *Nano Letters*, vol. 13, no. 9, pp. 4505–4510, 2013.

[27] D. Bi, S.-J. Moon, L. Häggman et al., "Using a two-step deposition technique to prepare perovskite $(CH_3NH_3PbI_3)$ for thin film solar cells based on ZrO_2 and TiO_2 mesostructures," *RSC Advances*, vol. 3, no. 41, pp. 18762–18766, 2013.

[28] S. H. Hwang, J. Roh, J. Lee, J. Ryu, J. Yun, and J. Jang, "Size-controlled SiO2 nanoparticles as scaffold layers in thin-film perovskite solar cells," *Journal of Materials Chemistry A*, vol. 2, no. 39, pp. 16429–16433, 2014.

[29] D. Liu and T. L. Kelly, "Perovskite solar cells with a planar heterojunction structure prepared using room-temperature solution processing techniques," *Nature Photonics*, vol. 8, no. 2, pp. 133–138, 2014.

[30] M. Liu, M. B. Johnston, and H. J. Snaith, "Efficient planar heterojunction perovskite solar cells by vapour deposition," *Nature*, vol. 501, no. 7467, pp. 395–398, 2013.

[31] H. Zhou, Q. Chen, and G. Li, "Interface engineering of highly efficient perovskite solar cells," *Science*, vol. 345, no. 6196, pp. 542–546, 2014.

[32] O. Malinkiewicz, A. Yella, Y. H. Lee et al., "Perovskite solar cells employing organic charge-transport layers," *Nature Photonics*, vol. 8, no. 2, pp. 128–132, 2014.

[33] Q. Wu, C. Xue, Y. Li et al., "Kesterite Cu2ZnSnS4 as a Low-Cost Inorganic Hole-Transporting Material for High-Efficiency Perovskite Solar Cells," *ACS Applied Materials & Interfaces*, vol. 7, no. 51, pp. 28466–28473, 2015.

[34] L. Xu, L.-L. Deng, J. Cao, X. Wang, W.-Y. Chen, and Z. Jiang, "Solution-Processed Cu(In, Ga)(S, Se)2 Nanocrystal as Inorganic Hole-Transporting Material for Efficient and Stable Perovskite Solar Cells," *Nanoscale Research Letters*, vol. 12, no. 1, article no. 159, 2017.

[35] C. Qi, H. Zhou, Z. Hong et al., "Planar heterojunction perovskite solar cells via vapor-assisted solution process," *Journal of the American Chemical Society*, vol. 136, no. 2, pp. 622–625, 2014.

[36] J. Chen, B.-X. Chen, F.-S. Zhang et al., "3,4-Phenylenedioxythiophene (PheDOT) Based Hole-Transporting Materials for Perovskite Solar Cells," *Chemistry - An Asian Journal*, vol. 11, no. 7, pp. 1043–1049, 2016.

[37] H. Jin, S. H. Im, J. H. Noh et al., "Efficient inorganic-organic hybrid heterojunction solar cells containing perovskite compound and polymeric hole conductors," *Nature Photonics*, vol. 7, no. 6, pp. 486–491, 2013.

[38] Q. Ping, Q. He, C. Chen et al., "High-performance rigid and flexible perovskite solar cells with low-temperature solution-processable binary metal oxide hole-transporting materials," *Solar RRL*, vol. 1, no. 8, p. 1700058, 2017.

[39] L.-Q. Ping, H.-W. Lei, X.-L. Zheng et al., "Copper-doped chromium oxide hole-transporting layer for perovskite solar cells: interface engineering and performance improvement," *Advanced Materials Interfaces*, vol. 3, no. 14, Article ID 1500799, 2016.

[40] J. Shi, J. Dong, S. Lv et al., "Hole-conductor-free perovskite organic lead iodide heterojunction thin-film solar cells: high efficiency and junction property," *Applied Physics Letters*, vol. 104, no. 6, Article ID 063901, 2014.

[41] H. Zhang, H. Wang, W. Chen, and A. K.-Y. Jen, "CuGaO2: A Promising Inorganic Hole-Transporting Material for Highly Efficient and Stable Perovskite Solar Cells," *Advanced Materials*, vol. 29, no. 8, Article ID 1604984, 2017.

[42] C. W. Chen, H. W. Kang, S. Y. Hsiao, P. F. Yang, K. M. Chiang, and H. W. Lin, "Efficient and uniform planar-type perovskite solar cells by simple sequential vacuum deposition," *Advanced Materials*, vol. 26, no. 38, pp. 6647–6652, 2014.

[43] J. J. Nam, J. H. Noh, Y. Kim, W. S. Yang, S. Ryn, and S. I. Seok, "Solvent engineering for high-performance inorganic-organic hybrid perovskite solar cells," *Nature Materials*, vol. 13, pp. 897–903, 2014.

[44] J.-W. Lee, D.-J. Seol, A.-N. Cho, and N.-G. Park, "High-efficiency perovskite solar cells based on the black polymorph of HC(NH2)2PbI3," *Advanced Materials*, vol. 26, no. 29, pp. 4991–4998, 2014.

[45] X. Jiang, Z. Yu, Y. Zhang et al., "High-Performance Regular Perovskite Solar Cells Employing Low-Cost Poly(ethylenedioxythiophene) as a Hole-Transporting Material," *Scientific Reports*, vol. 7, Article ID 42564, 2017.

[46] T. Matsui, J.-Y. Seo, M. Saliba, S. M. Zakeeruddin, and M. Grätzel, "Room-Temperature Formation of Highly Crystalline Multication Perovskites for Efficient, Low-Cost Solar Cells," *Advanced Materials*, vol. 29, no. 15, Article ID 1606258, 2017.

[47] A. Mei, X. Li, and L. Liu, "A hole-conductor-free, fully printable mesoscopic perovskite solar cell with high stability," *Science*, vol. 345, no. 6194, pp. 295–298, 2014.

[48] Y. Zhang, Y. Wang, Z. Sun et al., "Large grain growth for hole-conductor-free fully printable perovskite solar cells via polyoxometalate molecular doping," *Chemical Communications*, vol. 53, no. 14, pp. 2290–2293, 2017.

[49] H. Zhang, H. Wang, S. T. Williams et al., "SrCl2 Derived Perovskite Facilitating a High Efficiency of 16% in Hole-Conductor-Free Fully Printable Mesoscopic Perovskite Solar Cells," *Advanced Materials*, vol. 29, no. 15, Article ID 1606608, 2017.

[50] N. J. Jeon, J. H. Noh, W. S. Yang et al., "Compositional engineering of perovskite materials for high-performance solar cells," *Nature*, vol. 517, no. 7535, pp. 476–480, 2015.

[51] J. Liang, C. Wang, Y. Wang et al., "Correction to "All-Inorganic Perovskite Solar Cells"," *Journal of the American Chemical Society*, vol. 139, no. 7, pp. 2852-2852, 2017.

[52] A. Swarnkar, A. R. Marshall, E. M. Sanehira et al., "Quantum dot-induced phase stabilization of α-CsPbI3 perovskite for high-efficiency photovoltaics," *Science*, vol. 354, no. 6308, pp. 92–95, 2016.

[53] C. F. Lau, X. Deng, Q. Ma et al., " CsPbIBr ," *ACS Energy Letters*, vol. 1, no. 3, pp. 573–577, 2016.

[54] J. S. Niezgoda, B. J. Foley, A. Z. Chen, and J. J. Choi, " Improved Charge Collection in Highly Efficient CsPbBrI ," *ACS Energy Letters*, vol. 2, no. 5, pp. 1043–1049, 2017.

[55] J. K. Nam, S. U. Chai, W. Cha et al., "Potassium Incorporation for Enhanced Performance and Stability of Fully Inorganic Cesium Lead Halide Perovskite Solar Cells," *Nano Letters*, vol. 17, no. 3, pp. 2028–2033, 2017.

[56] S. A. Kulkarni, T. Baikie, P. P. Boix, N. Yantara, N. Mathews, and S. Mhaisalkar, "Band-gap tuning of lead halide perovskites using a sequential deposition process," *Journal of Materials Chemistry A*, vol. 2, no. 24, pp. 9221–9225, 2014.

[57] G. E. Eperon, S. D. Stranks, C. Menelaou, M. B. Johnston, L. M. Herz, and H. J. Snaith, "Formamidinium lead trihalide: a broadly tunable perovskite for efficient planar heterojunction solar cells," *Energy & Environmental Science*, vol. 7, no. 3, pp. 982–988, 2014.

[58] W. Zhu, C. Bao, F. Li et al., "An efficient planar-heterojunction solar cell based on wide-bandgap CH3NH3PbI2.1Br0.9 perovskite film for tandem cell application," *Chemical Communications*, vol. 52, no. 2, pp. 304–307, 2015.

[59] J. H. Noh, S. H. Im, J. H. Heo, T. N. Mandal, and S. I. Seok, "Chemical management for colorful, efficient, and stable inorganic-organic hybrid nanostructured solar cells," *Nano Letters*, vol. 13, no. 4, pp. 1764–1769, 2013.

[60] F. Brivio, C. Caetano, and A. Walsh, "Thermodynamic Origin of Photoinstability in the CH3NH3Pb(I1-xBrx)3 Hybrid Halide Perovskite Alloy," *The Journal of Physical Chemistry Letters*, vol. 7, no. 6, pp. 1083–1087, 2016.

[61] S. D. Stranks, G. E. Eperon, G. Grancini et al., "Electron-hole diffusion lengths exceeding 1 micrometer in an organometal trihalide perovskite absorber," *Science*, vol. 342, no. 6156, pp. 341–344, 2013.

[62] G. Xing, N. Mathews, and S. Sun, "Long-range balanced electron- and hole-transport lengths in organic-inorganic $CH_3NH_3PbI_3$," *Science*, vol. 342, pp. 344–347, 2013.

[63] P. Docampo, F. C. Hanusch, S. D. Stranks et al., "Solution deposition-conversion for planar heterojunction mixed halide perovskite solar cells," *Advanced Energy Materials*, vol. 4, no. 14, Article ID 1400355, 2014.

[64] E. Mosconi, E. Ronca, and F. De Angelis, "First-principles investigation of the TiO2/organohalide perovskites interface: The role of interfacial chlorine," *The Journal of Physical Chemistry Letters*, vol. 5, no. 15, pp. 2619–2625, 2014.

[65] B. Suarez, V. Gonzalez-Pedro, T. S. Ripolles, R. S. Sanchez, L. Otero, and I. Mora-Sero, "Recombination study of combined halides (Cl, Br, I) perovskite solar cells," *The Journal of Physical Chemistry Letters*, vol. 5, no. 10, pp. 1628–1635, 2014.

[66] C. Bi, Y. Yuan, Y. Fang, and J. Huang, "Perovskite Solar Cells: Low-Temperature Fabrication of Efficient Wide-Bandgap Organolead Trihalide Perovskite Solar Cells (Adv. Energy Mater. 6/2015)," *Advanced Energy Materials*, vol. 5, no. 6, 2015.

[67] C.-H. Chiang, J.-W. Lin, and C.-G. Wu, "One-step fabrication of a mixed-halide perovskite film for a high-efficiency inverted solar cell and module," *Journal of Materials Chemistry A*, vol. 4, no. 35, pp. 13525–13533, 2016.

[68] D. P. McMeekin, G. Sadoughi, W. Rehman et al., "A mixed-cation lead mixed-halide perovskite absorber for tandem solar cells," *Science*, vol. 351, no. 6269, pp. 151–155, 2016.

[69] C. Yi, J. Luo, S. Meloni et al., " Entropic stabilization of mixed A-cation ABX ," *Energy & Environmental Science*, vol. 9, no. 2, pp. 656–662, 2016.

[70] N. Pellet, P. Gao, G. Gregori et al., "Mixed-organic-cation perovskite photovoltaics for enhanced solar-light harvesting," *Angewandte Chemie International Edition*, vol. 53, no. 12, pp. 3151–3157, 2014.

[71] Y. Deng, Q. Dong, C. Bi, Y. Yuan, and J. Huang, "Air-Stable, Efficient Mixed-Cation Perovskite Solar Cells with Cu Electrode by Scalable Fabrication of Active Layer," *Advanced Energy Materials*, vol. 6, no. 11, Article ID 1600372, 2016.

[72] H. Choi, J. Jeong, H.-B. Kim et al., "Cesium-doped methylammonium lead iodide perovskite light absorber for hybrid solar cells," *Nano Energy*, vol. 7, pp. 80–85, 2014.

[73] G. Niu, W. Li, J. Li, X. Liang, and L. Wang, "Enhancement of thermal stability for perovskite solar cells through cesium doping," *RSC Advances*, vol. 7, no. 28, pp. 17473–17479, 2017.

[74] Y. H. Park, I. Jeong, S. Bae et al., " Solar Cells: Inorganic Rubidium Cation as an Enhancer for Photovoltaic Performance and Moisture Stability of HC(NH ," *Advanced Functional Materials*, vol. 27, no. 16, 2017.

[75] M. Zhang, J. S. Yun, Q. Ma et al., "High-Efficiency Rubidium-Incorporated Perovskite Solar Cells by Gas Quenching," *ACS Energy Letters*, vol. 2, no. 2, pp. 438–444, 2017.

[76] M. Kulbak, S. Gupta, N. Kedem et al., "Cesium Enhances Long-Term Stability of Lead Bromide Perovskite-Based Solar Cells," *The Journal of Physical Chemistry Letters*, vol. 7, no. 1, pp. 167–172, 2016.

[77] Q. Ma, S. Huang, X. Wen, M. A. Green, and A. W. Y. Ho-Baillie, "Hole Transport Layer Free Inorganic CsPbIBr2 Perovskite Solar Cell by Dual Source Thermal Evaporation," *Advanced Energy Materials*, vol. 6, no. 7, Article ID 1502202, 2016.

[78] R. E. Beal, D. J. Slotcavage, T. Leijtens et al., "Cesium Lead Halide Perovskites with Improved Stability for Tandem Solar Cells," *The Journal of Physical Chemistry Letters*, vol. 7, no. 5, pp. 746–751, 2016.

[79] Y. Ogomi, A. Morita, S. Tsukamoto et al., "$CH_3NH_3SnxPb_{(1-x)}I_3$ perovskite solar cells covering up to 1060 nm," *The Journal of Physical Chemistry Letters*, vol. 5, no. 6, pp. 1004–1011, 2014.

[80] F. Hao, C. C. Stoumpos, D. H. Cao, R. P. H. Chang, and M. G. Kanatzidis, "Lead-free solid-state organic-inorganic halide perovskite solar cells," *Nature Photonics*, vol. 8, no. 6, pp. 489–494, 2014.

[81] F. Hao, C. C. Stoumpos, R. P. H. Chang, and M. G. Kanatzidis, "Anomalous band gap behavior in mixed Sn and Pb perovskites enables broadening of absorption spectrum in solar cells," *Journal of the American Chemical Society*, vol. 136, no. 22, pp. 8094–8099, 2014.

[82] F. Zuo, S. T. Williams, P.-W. Liang, C.-C. Chueh, C.-Y. Liao, and A. K.-Y. Jen, "Binary-Metal Perovskites Toward High-Performance Planar-Heterojunction Hybrid Solar Cells," *Advanced Materials*, vol. 26, no. 37, pp. 6454–6460, 2014.

[83] N. K. Noel, S. D. Stranks, and A. Abate, "Lead-free organic-inorganic tin halide perovskites for photovoltaic applications," *Energy & Environmental Science*, vol. 7, no. 9, pp. 3061–3068, 2014.

[84] C. Liu, W. Li, H. Li, C. Zhang, J. Fan, and Y. Mai, " C ," *Nanoscale*, vol. 9, no. 37, pp. 13967–13975, 2017.

[85] K. P. Marshall, M. Walker, R. I. Walton, and R. A. Hatton, "Enhanced stability and efficiency in hole-transport-layer-free CsSnI3 perovskite photovoltaics," *Nature Energy*, vol. 1, p. 16178, 2016.

[86] T. Krishnamoorthy, H. Ding, C. Yan et al., "Lead-free germanium iodide perovskite materials for photovoltaic applications," *Journal of Materials Chemistry A*, vol. 3, no. 47, pp. 23829–23832, 2015.

[87] B.-W. Park, B. Philippe, X. Zhang, H. Rensmo, G. Boschloo, and E. M. J. Johansson, "Bismuth Based Hybrid Perovskites A3Bi2I9 (A: Methylammonium or Cesium) for Solar Cell Application," *Advanced Materials*, vol. 27, no. 43, pp. 6806–6813, 2015.

[88] X. Zheng, C. Wu, S. K. Jha, Z. Li, K. Zhu, and S. Priya, "Improved Phase Stability of Formamidinium Lead Triiodide Perovskite by Strain Relaxation," *ACS Energy Letters*, vol. 1, no. 5, pp. 1014–1020, 2016.

[89] M. Saliba, T. Matsui, J. Seo et al., "Cesium-containing triple cation perovskite solar cells: improved stability, reproducibility and high efficiency," *Energy & Environmental Science*, vol. 9, no. 6, pp. 1989–1997, 2016.

[90] M. Saliba, T. Matsui, K. Domanski et al., "Incorporation of rubidium cations into perovskite solar cells improves photovoltaic performance," *Science*, vol. 354, no. 6309, pp. 206–209, 2016.

[91] H. Li, W. Shi, W. Huang et al., " Carbon Quantum Dots/TiO ," *Nano Letters*, vol. 17, no. 4, pp. 2328–2335, 2017.

[92] X. Gao, J. Li, S. Gollon et al., "A TiO2 nanotube network electron transport layer for high efficiency perovskite solar cells," *Physical Chemistry Chemical Physics*, vol. 19, no. 7, pp. 4956–4961, 2017.

[93] K. Cao, J. Cui, H. Zhang et al., " Efficient mesoscopic perovskite solar cells based on the CH ," *Journal of Materials Chemistry A*, vol. 3, no. 17, pp. 9116–9122, 2015.

[94] Y. Yang, J. You, Z. Hong et al., "Low-temperature solution-processed perovskite solar cells with high efficiency and flexibility," *ACS Nano*, vol. 8, no. 2, pp. 1674–1680, 2014.

[95] F. Huang, A. R. Pascoe, W. Wu et al., "Perovskite Solar Cells: Effect of the Microstructure of the Functional Layers on the Efficiency of Perovskite Solar Cells (Adv. Mater. 20/2017)," *Advanced Materials*, vol. 29, no. 20, 2017.

[96] P. Docampo, J. M. Ball, M. Darwich, G. E. Eperon, and H. J. Snaith, "Efficient organometal trihalide perovskite planar-heterojunction solar cells on flexible polymer substrates," *Nature Communications*, vol. 4, article 2761, 2013.

[97] J. H. Noh, N. J. Jeon, Y. C. Choi, M. K. Nazeeruddin, M. Grätzel, and S. I. Seok, "Nanostructured $TiO_2/CH_3NH_3PbI_3$ heterojunction solar cells employing spiro-OMeTAD/Co-complex as hole-transporting material," *Journal of Materials Chemistry A*, vol. 1, no. 38, pp. 11842–11847, 2013.

[98] N. J. Jeon, J. H. Noh, Y. Kim, W. S. Yang, S. Ryn, and S. I. Seok, "Solvent engineering for high-performance inorganic-organic hybrid perovskite solar cells," *Nature Materials*, vol. 13, pp. 897–903, 2014.

[99] Y. Zhang, W. Liu, F. Tan, and Y. Gu, "The essential role of the poly(3-hexylthiophene) hole transport layer in perovskite solar cells," *Journal of Power Sources*, vol. 274, pp. 1224–1230, 2015.

[100] Y. Yang, J. You, Z. Hong et al., "Low-temperature solution-processed perovskite solar cells with high efficiency and flexibility," *ACS Nano*, vol. 8, no. 2, pp. 1674–1680, 2014.

[101] J. A. Christians, R. C. M. Fung, and P. V. Kamat, "An inorganic hole conductor for Organo-lead halide perovskite solar cells. improved hole conductivity with copper iodide," *Journal of the American Chemical Society*, vol. 136, no. 2, pp. 758–764, 2014.

[102] S. Seo, I. J. Park, M. Kim et al., "An ultra-thin, un-doped NiO hole transporting layer of highly efficient (16.4%) organic-inorganic hybrid perovskite solar cells," *Nanoscale*, vol. 8, no. 22, pp. 11403–11412, 2016.

[103] P. Qin, S. Tanaka, S. Ito et al., "Inorganic hole conductor-based lead halide perovskite solar cells with 12.4% conversion efficiency," *Nature Communications*, vol. 5, article 3834, 2014.

[104] T. Minemoto and M. Murata, "Impact of work function of back contact of perovskite solar cells without hole transport material analyzed by device simulation," *Current Applied Physics*, vol. 14, no. 11, pp. 1428–1433, 2014.

[105] T. Wang, J. Chen, G. Wu, and M. Li, "Optimal design of efficient hole transporting layer free planar perovskite solar cell," *Science China Materials*, vol. 59, no. 9, pp. 703–709, 2016.

[106] Z. Li, S. A. Kulkarni, and P. P. Boix, "Laminated carbon nanotube networks for metal electrode-free efficient perovskite solar cells," *ACS Nano*, vol. 8, no. 7, pp. 6797–6804, 2014.

[107] A. Djurišić, F. Liu, H. Tam et al., "Perovskite solar cells - An overview of critical issues," *Progress in Quantum Electronics*, vol. 53, pp. 1–37, 2017.

[108] J. L. Barnett, V. L. Cherrette, C. J. Hutcherson, and M. C. So, "Effects of Solution-Based Fabrication Conditions on Morphology of Lead Halide Perovskite Thin Film Solar Cells," *Advances in Materials Science and Engineering*, vol. 2016, Article ID 4126163, 2016.

[109] K. Liang, D. B. Mitzi, and M. T. Prikas, "Synthesis and characterization of organic–inorganic perovskite thin films prepared using a versatile two-step dipping technique," *Chemistry of Materials*, vol. 10, no. 1, pp. 403–411, 1998.

[110] Y. Xu, L. Zhu, J. Shi et al., "The Effect of Humidity upon the Crystallization Process of Two-Step Spin-Coated Organic-Inorganic Perovskites," *ChemPhysChem*, vol. 17, no. 1, pp. 112–118, 2016.

[111] D. Forgács, L. Gil-Escrig, D. Pérez-Del-Rey et al., "Efficient Monolithic Perovskite/Perovskite Tandem Solar Cells," *Advanced Energy Materials*, vol. 7, no. 8, 2017.

[112] Q. Chen, H. Zhou, Z. Hong et al., "Planar heterojunction perovskite solar cells via vapor-assisted solution process," *Journal of the American Chemical Society*, vol. 136, no. 2, pp. 622–625, 2014.

[113] G. Peng, X. Xu, and G. Xu, "Hybrid Organic-Inorganic Perovskites Open a New Era for Low-Cost, High Efficiency Solar Cells," *Journal of Nanomaterials*, vol. 2015, Article ID 241853, 10 pages, 2015.